Vietnam Journal of Science and Technology ***57*** *(4A) (2019) 51-60*

doi:10.15625/2525-2518/57/4A/14013

VIBRATION OF FGSW BEAMS UNDER NONUNIFORM MOTION OF MOVING LOAD USING AN EFFICIENT THIRD-ORDER SHEAR DEFORMATION FINITE ELEMENT FORMULATION

Le Thi Ngoc Anh[1, 2, *], Nguyen Dinh Kien[2, 3]

[1]*Institute of Applied Information and Mechanics, 291 Dien Bien Phu, HCMC, Viet Nam*
[2]*Graduate University of Science and Technology, VAST 18 Hoang Quoc Viet, Ha Noi, Viet Nam*
[3]*Institute of Mechanics, VAST, 18 Hoang Quoc Viet, Ha Noi, Viet Nam*

[*]Email: *lengocanhkhtn@gmail.com*

Received: 23 July 2019; Accepted for publication: 9 November 2019

Abstract. Vibration of functionally graded sandwich (FGSW) beams under nonuniform motion of a moving load is studied using a third-order shear deformation finite element formulation. The beams consists of three layers, a homogeneous ceramic core and two functionally graded faces. Instead of the rotation, the finite element formulation is derived by using the transverse shear rotation as an unknown. Newmark method is used to compute the dynamic response of the beams. Numerical result reveals that the derived formulation is efficient, and it is capable to give accurate vibration characteristics by a small number of the elements. A parametric study is carried out to illustrate the effects of the material distribution, layer thickness ratio and moving load speed on the dynamic behavior of the beams. The influence of acceleration and deceleration of the moving load on the vibration of the beams is also examined and discussed.

Keywords: FGSW beam, moving load, third-order shear deformation theory, transverse shear rotation, vibration**.**

Classification numbers: 2.9.4, 5.4.2, 5.4.3.

1. INTRODUCTION

Functionally graded material (FGM) has widely employed to fabricate structural elements for using in industries. With the development in the manufacturing methods [1], FGMs can be incorporated in the sandwich construction to improve performance of the structural components. Investigations on mechanical vibration of functionally graded sandwich (FGSW) beams, the topic discussed in this paper, have been extensively reported in recent years. In this line of works, Pradhan and Murmu [2] employed the modified differential quadrature method to compute the natural frequencies of FGSW beams formed from an Alporas foam core and two FGM skin layer. Amirani *et al*. [3] studied free vibration of FGSW beam with a functionally graded core with the aid of the element free Galerkin method. Based on Reddy-Birkford shear deformation theory, Vo *et al*. [4] presented a finite element model for free vibration and buckling analyses of FGSW beams. The thickness stretching effect is then included into the theory by the authors in the analysis of FGSW beams [5]. A hyperbolic shear deformation beam theory was used by Bennai *et al*. [6] to study free vibration and buckling of FGSW beams. Trinh *et al*. [7] evaluated the fundamental frequencies of FGSW beams by using the state space approach. The modified Fourier series method was adopted by Su *et al.* [8] to study free vibration of FGSW beams resting on a Pasternak foundation. A finite element formulation based on hierarchical displacement field was derived by Mashat *et al*. [9] for evaluating natural frequencies of laminated and sandwich beams. The accuracy and efficiency of the formulation were shown through the numerical investigation.

Vibration of structures excited by moving has wide application in engineering. With the invention of FGMs, the vibration of FGM beams due to moving loads has drawn attention from researchers recently. Şimşek and his co-workers [10, 11] approximated the displacement field by polynomials to compute dynamic response of FGM beams under a moving load. Lagrange multiplayer method has been employed to handle the boundary conditions. The method is then extended to study vibration of FGSW beams subjected to two moving harmonic loads [12]. Rayleigh-Ritz method was used by Khalili *et al*. [13] to study dynamic behavior of FGM Euler-Bernoulli beams under moving load. Vibration of an FGM Euler-Bernoulli beam due to a moving oscillator was investigated in [14] by the Runge-Kutta method. Finite element method has been also used to study vibration of FGM beams excited by moving loads [15, 16].

It is clear from the above literature review that only Ref. [12] deals with vibration of FGSW Timoshenko beams under two moving harmonic loads. This topic is explored some more further in this paper by using the finite element method. The beams considered herein consists of three layers, a homogeneous ceramic core and two functionally graded faces. A third-order shear deformable finite element formulation in which the transverse shear rotation rather than the rotation is employed as an independent unknown is derived and used in combination with Newmark method to compute the dynamic response of the beams. The effects of material distribution, moving load speed and layer thickness ratio the beams on vibration characteristics are examined. The influence of acceleration and deceleration of the moving load on the dynamic behavior of the beams is also examined and highlighted.

2. FGSW BEAMS AND MATHEMATICAL MODEL

2.1. FGSW Beam

A simply supported FGSW beam with length *L*, rectangular cross section, under a load Q_0, moving from left to right as shown in Figure 1 is considered. In addition to the constant speed, acceleration and deceleration of the moving load is also considered herein.

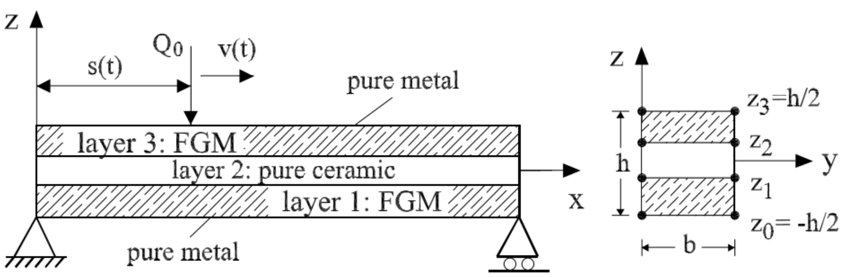

Figure 1. FGSW beam under a moving load.

The beam is assumed to consist three layers, namely a homogeneous ceramic core and two ceramic-metal FGM layers. Denoting z_0, z_1, z_2, z_3, in which $z_0 = -h/2, z_3 = h/2$, are the vertical coordinates of the bottom surface, interfaces and top face, respectively. The volume fraction of ceramic and metal are varied in the thickness according to [4, 5]

$$V_c = \begin{cases} \left(\dfrac{z - z_0}{z_1 - z_0}\right)^n & \text{for} \quad z \in [z_0, z_1] \\ 1 & \text{for} \quad z \in [z_1, z_2] \\ \left(\dfrac{z - z_3}{z_2 - z_3}\right)^n & \text{for} \quad z \in [z_2, z_3] \end{cases} \tag{1}$$

and

$$V_m + V_c = 1, \tag{2}$$

with V_c and V_m, respectively, are the volume fraction of ceramic and metal; n is the material index, defining the variation of the constituents in the thickness direction.

The effective property $P(z)$, evaluated by Voigt's model, is of the form

$$P(z) = \begin{cases} (P_c - P_m)\left(\dfrac{z - z_0}{z_1 - z_0}\right)^n + P_m & \text{for} \quad z \in [z_0, z_1] \\ P_c & \text{for} \quad z \in [z_1, z_2] \\ (P_c - P_m)\left(\dfrac{z - z_3}{z_2 - z_3}\right)^n + P_m & \text{for} \quad z \in [z_2, z_3] \end{cases} \tag{3}$$

where, P_c and P_m are the properties of the ceramic and metal, respectively.

2.2. Mathematical model

The displacements in the x- and z-directions based on the third-order shear deformation proposed recently by Shi [17] are given by

$$u(x,z,t) = u_0(x,t) + \frac{1}{4} z\left(5\theta + w_{0,x}\right) - \frac{5}{3h^2} z^3\left(\theta + w_{0,x}\right), \quad w(x,z,t) = w_0(x,t) \tag{4}$$

where $u_0(x,t), w_0(x,t)$ are, respectively, the axial and transverse displacements of a point on the x- axis; t is the time variable, and θ is the cross-sectional rotation.

Using a notation for a transverse shear rotation γ_0, defined as

$$\gamma_0 = \theta + w_{0,x}, \tag{5}$$

Equation (4) can be rewritten in the following form

$$u(x,z,t) = u_0(x,t) + z\left(\frac{5}{4}\gamma_0 - w_{0,x}\right) - \frac{5}{3h^2} z^3\gamma_0, \quad w(x,t) = w_0(x,t) \tag{6}$$

The axial strain and shear strain resulted from equation (6) are

$$\varepsilon_{xx} = u_{0,x} + z\left(\frac{5}{4}\gamma_{0,x} - w_{0,xx}\right) - \frac{5}{3h^2}z^3\gamma_{0,x}, \quad \gamma_{zx} = 5\left(\frac{1}{4} - \frac{z^2}{h^2}\right)\gamma_0 \tag{7}$$

Based on the Hooke's law, the axial and shear stresses, σ_{xx} and τ_{xz}, are of the form

$$\sigma_{xx} = E(z)\varepsilon_{xx}, \ \ \tau_{xz} = G(z)\gamma_{xz} \tag{8}$$

The strain energy (U) and the kinetic energy (T) of the FGSW beam are then given by

$$U = \frac{1}{2}\int_0^L\int_A \left(\sigma_{xx}\varepsilon_{xx} + \gamma_{zx}\tau_{xz}\right)dAdx, \quad T = \frac{1}{2}\int_0^L\int_V \rho(z)\left(\dot{u}^2 + \dot{w}^2\right)dAdx \tag{9}$$

where $A = bh$ is the cross-sectional area, and $\rho(z)$ is the mass density.

From Eqs. (7) and (8), the strain energy can be written as

$$\begin{aligned} U = \frac{1}{2}\int_0^L \Bigg[& A_{11}u_{0,x}^2 + 2A_{12}u_{0,x}\left(\frac{5}{4}\gamma_{0,x} - w_{0,xx}\right) + A_{22}\left(\frac{5}{4}\gamma_{0,x} - w_{0,xx}\right)^2 - \frac{10}{3h^2}A_{34}u_{0,x}\gamma_{0,x} \\ & - \frac{10}{3h^2}A_{44}\gamma_{0,x}\left(\frac{5}{4}\gamma_{0,x} - w_{0,xx}\right) + \frac{25}{9h^4}A_{66}\gamma_{0,x}^2 + 25\left(\frac{1}{16}B_{11} - \frac{1}{2h^2}B_{22} + \frac{1}{h^4}B_{44}\right)\gamma_0^2\Bigg]dx \end{aligned} \tag{10}$$

and the kinetic energy resulted from Eq. (6) is as follow

$$\begin{aligned} T = \frac{1}{2}\int_0^L \Bigg[& I_{11}\left(\dot{u}_0^2 + \dot{w}_0^2\right) + 2I_{12}\dot{u}_0\left(\frac{5}{4}\dot{\gamma}_0 - \dot{w}_{0,x}\right) + I_{22}\left(\frac{5}{4}\dot{\gamma}_0 - \dot{w}_{0,x}\right)^2 \\ & - \frac{10}{3h^2}I_{34}\dot{u}_0\dot{\gamma}_0 - \frac{10}{3h^2}I_{44}\dot{\gamma}_0\left(\frac{5}{4}\dot{\gamma}_0 - \dot{w}_{0,x}\right) + \frac{25}{9h^4}I_{66}\dot{\gamma}_0^2\Bigg]dx \end{aligned} \tag{11}$$

In Eq. (10), A_{ij} and B_{ij} $(i, j = 1, 2, 3, 4, 5, 6)$ are the beam rigidities, defined as

$$(A_{11}, A_{12}, A_{22}, A_{34}, A_{44}, A_{66}) = \int_A E^k(z)(1, z, z^2, z^3, z^4, z^6)\,dA \tag{12}$$

$$(B_{11}, B_{22}, B_{44}) = \int_A G^k(z)(1, z^2, z^4)dA \tag{13}$$

and I_{ij} in Eq (11) are the mass moments, defined as

$$(\mathrm{I}_{11}, I_{12}, I_{22}, I_{34}, I_{44}, I_{66}) = \int_A \rho^k(z)(1, z, z^2, z^3, z^4, z^6)\,dA \tag{14}$$

In the above equations, $E^k(z), G^k(z),$ and are, respectively, the elastic modulus, shear modulus and mass density of the k^{th} layer.

The potential energy of the moving load $\rho^k(z)$ is simply given by

$$V = -Q_0 w(x,t)\delta(x - s(t)) \tag{15}$$

where $\delta(.)$ is the Dirac delta function, and $s(t)$ is the function expressing the motion of the load Q_0, and it can be expressed through speed at left end (v_0) and acceleration a of the load Q_0 as

$$s(t) = v_0 t + \frac{1}{2}at^2, \tag{16}$$

The acceleration a is assumed to be constant in the present study. With $a = 0$, $a > 0$ and $a < 0$, the motion is uniform, accelerated and decelerated, respectively.

3. FINITE ELEMENT FORMULATION

Assuming the beam is being divided into $nELE$ elements with length of l. The vector of nodal displacements for a standard two-node beam element, (i, j), herein is given by

$$\mathbf{d} = \left\{ u_i \quad w_i \quad w_{xi} \quad \gamma_i \quad u_j \quad w_j \quad w_{xj} \quad \gamma_j \right\}^T \tag{17}$$

where u_i, w_i, w_{xi} and γ_i are the values of $u_0, w_0, w_{0,x}$ and γ_0 at the node i; u_j, w_j, w_{xj} and γ_j are the corresponding values of these quantities at the node j. The superscript "T" in Eq. (17) and hereafter is used to indicate the transpose of a vector or a matrix.

The displacements $u_0(x,t)$, $w_0(x,t)$ and the shear deformation $\gamma_0(x,t)$ are interpolated as

$$u_0 = \mathbf{N}_u^T \mathbf{d}, \qquad w_0 = \mathbf{N}_w^T \mathbf{d}, \qquad \gamma_0 = \mathbf{N}_\gamma^T \mathbf{d}, \tag{18}$$

with $\mathbf{N}_u, \mathbf{N}_w$, and $\mathbf{N}_\gamma$ are the matrices of interpolating functions. Linear functions are employed for the u_0, γ_0, while cubic Hermite polynomials are employed for w_0 herein. Based on Eq. (18), one can write the strain and kinetic energies in Eqs. (10) and (11) in the forms

$$U = \frac{1}{2} \sum_{i=1}^{nELE} \mathbf{d}^T \mathbf{k}\, \mathbf{d}\,, \quad T = \frac{1}{2} \sum_{i=1}^{nELE} \mathbf{d}^T \mathbf{m}\, \mathbf{d} \tag{19}$$

with the element stiffness and mass matrices $\mathbf{k}$ and $\mathbf{m}$ can be written in the forms

$$\mathbf{k} = \mathbf{k}_{11} + \mathbf{k}_{12} + \mathbf{k}_{22} + \mathbf{k}_{34} + \mathbf{k}_{44} + \mathbf{k}_{66} \tag{20}$$

$$\mathbf{m} = \mathbf{m}_{11} + \mathbf{m}_{12} + \mathbf{m}_{22} + \mathbf{m}_{34} + \mathbf{m}_{44} + \mathbf{m}_{66} \tag{21}$$

where

$$\begin{aligned}
&\mathbf{k}_{11} = \int_0^l N_{u,x}^T A_{11} N_{u,x} dx; \; \mathbf{k}_{12} = \int_0^l N_{u,x}^T A_{12} \left(N_{\gamma,x} - N_{w,xx} \right) dx; \\
&\mathbf{k}_{22} = \int_0^l \left(N_{\gamma,x} - N_{w,xx} \right)^T A_{22} \left(N_{\gamma,x} - N_{w,xx} \right) dx; \quad \mathbf{k}_{34} = \int_0^l N_{u,x}^T A_{34} N_{\gamma,x} dx; \\
&\mathbf{k}_{44} = \int_0^l N_{\gamma,x}^T A_{44} \left(N_{\gamma,x} - N_{w,xx} \right) dx; \; \mathbf{k}_{66} = \int_0^l N_{\gamma,x}^T A_{66} N_{\gamma,x} dx.
\end{aligned} \tag{22}$$

and

$$\begin{aligned}
&\mathbf{m}_{11} = \int_0^l \left(N_u^T I_{11} N_u + N_w^T I_{11} N_w \right) dx; \; \mathbf{m}_{12} = \int_0^l N_u^T I_{12} \left(N_\gamma - N_{w,x} \right) dx; \\
&\mathbf{m}_{22} = \int_0^l \left(N_\gamma - N_{w,x} \right)^T I_{22} \left(N_\gamma - N_{w,x} \right) dx; \quad \mathbf{m}_{34} = \int_0^l N_u^T I_{34} N_\gamma dx; \\
&\mathbf{m}_{44} = \int_0^l N_\gamma^T I_{44} \left(N_\gamma - N_{w,x} \right) dx; \quad \mathbf{m}_{66} = \int_0^l N_\gamma^T I_{66} N_\gamma dx.
\end{aligned} \tag{23}$$

The equations of motion for the beam in the discrete form is as follows

$$\mathbf{M}\ddot{\mathbf{D}} + \mathbf{K}\mathbf{D} = \mathbf{F}^{ex} \tag{24}$$

where $\mathbf{D}$, $\mathbf{M}$ and $\mathbf{K}$ are, respectively, the structural displacement vector, mass and stiffness matrices; the $\mathbf{F}^{ex}$ is the external nodal load vector which can be easily obtained from the potential energy (15) and the interpolation for w_0.

4. NUMERICAL RESULTS

A simply supported FGSW beam with (bxh)= (0.5m x 1m), formed from Alumina (Al_2O_3) and stainless steel (SUS304) is adopted in this section. The material data of the constituents are: E_c= 390MPa, ρ_c=3960 kg/m^3, ν_c=0.3 for Al_2O_3 ; E_m=210MPa, ρ_m=7800 kg/m^3, ν_m=0.3 for SUS304. Three numbers in the brackets introduced in Ref. [4, 5] are used herein to denote the layer thickness ratio. For example, (2-1-1) means that $(h_1 : h_2 : h_3)$ = (2-1-1). The amplitude of the moving load is taken as $Q_0 = 100$ kN.

It is assumed that for the acceleration the load enters the beam with a speed of zero, and it exits the beam with a speed of v, while these values are, respectively, v and 0 for the deceleration. Eq. (16) gives a total time ΔT necessary for the load to across the beam is L/v for the uniform motion, where this value is $2L/v$ for the accelerated and decelerated motions. A total of 500 time steps are used for the Newmark method.

The dynamic deflection factor f_D is introduced as

$$f_D = \max\left(\frac{w(L/2,t)}{w_0}\right) \tag{25}$$

where $w_0 = Q_0 L^3 / 48 E_m I$ is the maximum static deflection of the uniform steel beam.

4.1. Formulation verification

Table 1 compares the non-dimensional frequencies of the FGSW beam with L/h=20 obtained in the present work with that of Ref. [4] for various values of the layer thickness ratio. Very good agreements between the result of the present work with that of Ref. [4] is noted form Table 1. The non-dimensional frequency in Table 1 is defined according to [4]

$$\mu = \frac{\omega L^2}{h}\sqrt{\frac{\rho_m}{E_m}} \tag{26}$$

where ω is the fundamental frequency of the beam. It is noted that the frequencies Table 1 have converged by using just 20 elements, and this number of the element is used below.

Table 1. Comparison the non-dimensional fundamental frequency of FGSW beam (L/h = 20).

	(2-1-2)		(2-1-1)		(1-1-1)		(2-2-1)	
n	Present	Ref. [4]	Present	Ref. [4]	Present	Ref. [4]	Present	Ref. [4]
0.5	4.4315	4.4290	4.4990	4.4970	4.5345	4.5324	4.6187	4.6170
1	3.8785	3.8768	3.9789	3.9774	4.0343	4.0328	4.1614	4.1602
2	3.3476	3.3465	3.4765	3.4754	3.5398	3.5389	3.7058	3.7049
5	2.9315	2.9310	3.0781	3.0773	3.1115	3.1111	3.3034	3.3028

Table 2 lists the maximum dynamic deflection at the mid-span of the FGM beam under a constant moving load, where the result obtained by Şimşek and Kocatürk [10] is also given. The maximum deflections the present work are in good agreement with that of Ref. [10] is noted from Table 2. Noting that the result is Table 2 has been obtained with the data of Ref. [10].

Table 2. Comparison of maximum mid-span deflection of FGM beam under uniform motion.

n	0.2	0.5	1	2	SUS304	Al2O3
Present	1.0407	1.1508	1.2570	1.3449	1.7329	0.9382
Ref. [10]	1.0344	1.1444	1.2503	1.3376	1.7326	0.9382

4.2. Effect of layer thickness ratio

Tables 3 and 4 list values of the dynamic deflection factor f_D for the beam under different types of motion for L/h = 5 and L/h = 20, respectively. The tables show a significant influence of the layer thickness ratio and the grading index on the factor f_D, and f_D increases with an increase in the index n. By comparing the tables, one can see that the increase of f_D by increasing n is more significant for the beam with a lower aspect ratio, irrespective of the layer thickness ratio.

Table 3. Dynamic deflection factor f_D of FGSW beam under different motion type (L/h=5).

	n	(1-0-1)	(2-1-2)	(1-1-1)	(2-2-1)	(1-2-1)
$a = 0$	0.5	0.8391	0.8020	0.7902	0.7788	0.7670
	1	0.9895	0.9351	0.8873	0.8499	0.8218
	2	1.1018	1.057	1.0058	0.9579	0.9147
	5	1.1561	1.1364	1.0975	1.0472	1.0068
$a = 250$	0.5	0.8582	0.8170	0.8052	0.7915	0.7678
	1	0.9707	0.9448	0.9075	0.8666	0.8360
	2	1.1025	1.0328	0.9921	0.9652	0.9352
	5	1.1708	1.1058	1.0838	1.0233	0.9996
$a = -250$	0.5	0.8257	0.7998	0.7769	0.7626	0.7475
	1	0.9460	0.9033	0.8675	0.8416	0.8171
	2	1.0598	1.0027	0.9634	0.9238	0.8919
	5	1.1403	1.097	1.0463	0.9980	0.9662

The increase of the factor f_D is, however influenced by the motion type, and as can be seen from the tables, the factor f_D increases more significantly in the uniform and decelerated motions than it does in the accelerated motion. The influence of the index n and the layer thickness ratio on the factor f_D can also be seen from Figure 2, where the relation between the factor f_D and the moving load speed v is depicted for the beam with an aspect ratio L/h = 20 under uniform motion of the moving load and for different values of the index n and the layer thickness ratio.

Regardless of the moving load speed, the parameter f_D increases with an increase of the index *n* and it decreases with the increase of the core thickness.

Table 4. Dynamic deflection factor f_D of FGSW beam under different motion type (*L/h* = 20).

	n	(1-0-1)	(2-1-2)	(1-1-1)	(2-2-1)	(1-2-1)
	0.5	1.0116	0.9551	0.9114	0.8804	0.8497
a = 0	1	1.241	1.1554	1.0848	1.032	0.9828
	2	1.4568	1.3586	1.2682	1.1918	1.1268
	5	1.6042	1.5259	1.4344	1.3387	1.2699
	0.5	0.7406	0.7093	0.6938	0.6835	0.6758
	1	0.8973	0.8408	0.7923	0.7556	0.8219
a = 250	2	1.0237	0.9718	0.9177	0.8663	0.8217
	5	1.0045	1.0651	1.0183	0.9613	0.920
	0.5	0.9521	0.8984	0.8568	0.8272	0.7977
	1	1.1742	1.090	1.0215	0.971	0.9243
a = - 250	2	1.3882	1.2882	1.199	1.1248	1.0617
	5	1.5401	1.4562	1.3629	1.2682	1.2002

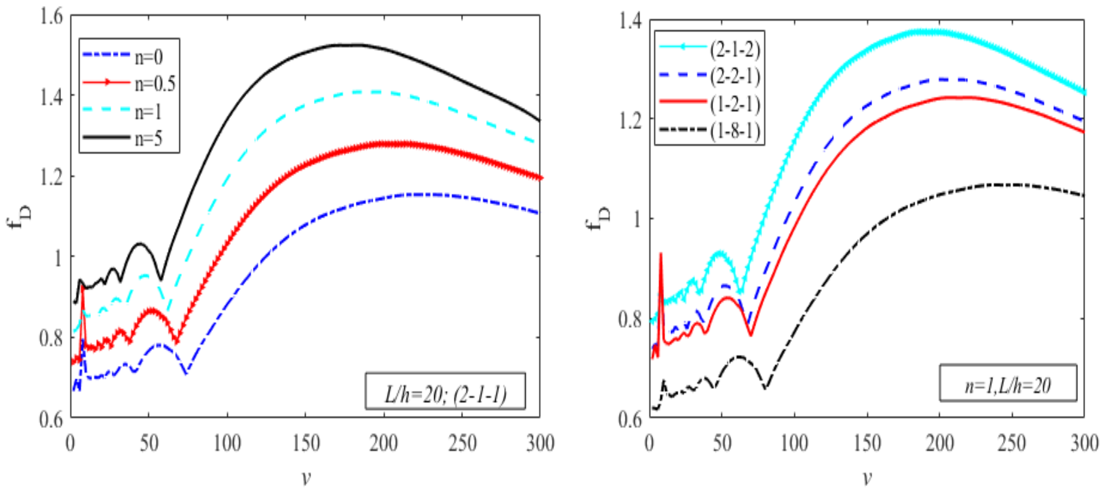

Figure 2. Relation between f_D and speed *v* of FGSW beam with *L*/*h* = 20 under uniform motion; Left: (2-1-1) beam with *n* variable, Right: beam with *n* = 1 and layer thickness variable.

4.3. Effect of acceleration and deceleration

The effect of the accelerated and decelerated motions is shown in Figure 3, where the relation between the dynamic deflection factor f_D and moving speed *v* is shown for the beam with *L/h* = 20 and *n* = 1 under different types of the motion. For the most values of the moving load speed, the factor f_D of the beam under the accelerated motion of the moving load is much lower than that of the beam under the other motions. Interestingly, the deceleration leads to the highest value of the factor f_D. The motion type does not only change the amplitude of the dynamic deflection factor f_D, but it also alters the speed at which the dynamic deflection factor attains the peak value. The peak value of the factor f_D in the decelerated motion is much higher that that in the uniform and accelerated motion, and it attains at a much higher moving load speed.

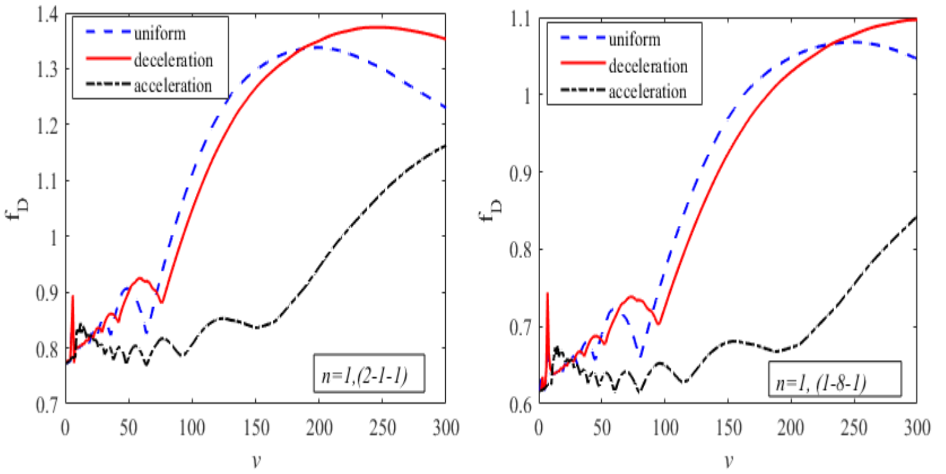

Figure 3. Relation between dynamic deflection factor and moving speed of FGSW beam under different motion types of moving load.

5. CONCLUSIONS

The vibration of a FGSW beam under nonuniform motion of a moving load has been investigated by using a third-order shear deformation finite element formulation. The transverse shear rotation rather than the cross-sectional rotation was used as a unknown in the derivation of the finite element formulation. Numerical result has confirmed the accuracy and the fast convergence of the derived formulation. The effects of the material distribution, layer thickness ratio and moving load speed on the dynamic behavior of the FGSW beam have been examined and highlighted. The obtained numerical results reveal that the dynamic response of the beams is governed by the moving speed, and also by the material and geometric parameter of the beam. The acceleration and deceleration of the moving load play an important role on the dynamic behavior of the beam, and the dynamic deflection factor obtained in the decelerated motion of the moving load is always higher than that obtained in the accelerated motion.

Acknowledgements. The work described in this article was supported by Vietnam National Foundation for Science and Technology Development (NAFOSTED), Grant no. 107.02-2018.23.

REFERENCES

1. Lambros J., Santare M. H., Li H., and Sapna G. H. - A novel technique for the fabrication of laboratory scale model of FGM, Experimental Mechanics **39** (1999) 184-190.
2. Pradhan S. C., and Murmu T. - Thermo-mechanical vibration of FGM sandwich beam under variable elastic foundations using differential quadrature method, Journal of Sound and Vibration **321** (2009) 342-362.

3. Amirani M. C., Khalili S. M. R., and Nemati N. - Free vibration analysis of sandwich beam with FG core using the element free Galerkin method, Composite Structures **90** (2009) 373-379.
4. Vo T. P., Thai H.-T., Nguyen T.-K., Maheri A., and Lee J. - Finite element model for vibration and buckling of functionally graded sandwich beams based on a refined shear deformation theory, Engineering Structures **64** (2014) 12-22.
5. Vo T. P., Thai H.-T., Nguyen T..K., Inam F., and Lee J. - A quasi-3D theory for vibration and buckling of functionally graded sandwich beams, Composite Structures **119** (2015) 1-12.
6. Bennai R., Atmane H. A., and Tounsi A. - A new higher-order shear and normal deformation theory for functionally graded sandwich beams, Steel and Composite Structures **19** (2015) 521-546.
7. Trinh L. C., Vo T. P., Osofero A. I., and Lee J. - Fundamental frequency analysis of functionally graded sandwich beams based on the state space approach, Composite Structures **156** (2016) 263-275.
8. Su Z., Jin G., Wang Y., and Ye X. - A general Fourier formulation for vibration analysis of functionally graded sandwich beams with arbitrary boundary condition and resting on elastic foundations, Acta Mechanica **227** (2016) 1493-1514.
9. Mashat D. S., Carrera E., Zenkour A. M., Al Khateeb S. A., and Filippi M. - Free vibration of FGM layered beams by various theories and finite elements, Composites: Part B, **59** (2014) 269-278.
10. Şimşek M., and Kocatürk, T. - Free and forced vibration of a functionally graded beam subjected to a concentrated moving harmonic load, Composite Structures **90** (2009) 465–473.
11. Şimşek M. - Vibration analysis of a functionally graded beam under a moving mass by using different beam theories, Composite Structures **92** (2010) 904-917.
12. Şimşek M., and Al-Shujairi M. - Static, free and forced vibration of functionally graded (FG) sandwich beams excited by two successive moving harmonic loads, Composite: Part B **108** (2017) 18-34.
13. Khalili S. M. R., Jafari A. A., and Eftekhari S. A. - A mixed Ritz-DQ method for forced vibration of functionally graded beams carrying moving loads, Composite Structures **92** (2010) 2497-2511.
14. K. Rajabi · M. H. Kargarnovin · M. Gharini - Dynamic analysis of a functionally graded simply supported Euler-Bernoulli beam subjected to a moving oscillator, Acta Mechanica **224** (2013) 425-446.
15. Gan B. S., Trinh T. H., Le T. H., Nguyen D. K. - Dynamic response of non-uniform Timoshenko beams made of axially FGM subjected to multiple moving point loads, Structural Engineering and Mechanics **53** (2015) 981-995.
16. Nguyen D. K., and Bui V. T. - Dynamic analysis of functionally graded Timoshenko beams in thermal environment using a higher-order hierarchical beam element, Mathematical Problems in Engineering (2017) https://doi.org/10.1155/2017/7025750
17. Shi G. - A new simple third-order shear deformation theory of plates, International Journal of Solids and Structures, **44** (2007) 4399-4417.